Stretch reflex improves rolling stability during hopping of a decerebrate system

Andre Rosendo, Xiangxiao Liu, Masahiro Shimizu and Koh Hosoda

Graduate School of Information Science and Technology, Osaka University, Osaka, Japan

E-mail: andre.rosendo@ist.osaka-u.ac.jp

Abstract. When humans hop, attitude recovery can be observed in both sagittal and frontal planes. While it is agreed that the brain plays an important role on leg placement, the role of low-level feedback (stretch reflex) on frontal plane stabilisation remains unclear. Aiming to better understand stretch reflex contribution to rolling stability, we performed experiments on a biomimetic humanoid hopping robot. Different reflex responses were used upon touching the floor, ranging from no response to long muscle activations, and the effect of a delay upon touching the floor was also observed. We found that the presence of stretch reflex brought the system closer to a stable, straight hopping. The presence of an activation delay did not affect the results, where both cases (with or without delay) outperformed the case without reflex response. Therefore, these results emphasise the importance of low-level control on locomotion, where the body stabilisation does not require brain created signals.

1. Introduction

Understanding how animals move has been the main objective of several researches in the past 100 years[1]. Through nature observation, biologists have been learning about animal locomotion [2, 3, 4], and recently, roboticists have been trying to replicate animal behaviour [5, 6, 7, 8] in an attempt to grasp the source of locomotion's stability.

Hitherto, it is understood that animals control their bodies through a combination of higher-level and lower-level control signals [9]. The former is originated from the brain and has a longer travelling distance to the actuator (muscle), having longer delays (above 300 ms for visual stimulus-manual response trials [10]), being the latter a stretch reflex response, created by muscle spindles upon sensing length changes on the muscle fibre. This response, faster than brain signals (below 50 ms) [11], has come to attention of researchers for its positive effects on body stability. In [12, 13], a decerebrated cat walking on a treadmill uses stretch reflex to stabilise its walking pattern, while in [14] feedback role on high-frequency walking of insects is explained.

Experiments have proven benefits from muscle feedback, caused by length changes (proprioception), on human standing stability [15, 16]. During human walking,

stretch reflex contributes to ankle extensor activation during early stance phase [17]. Moreover, biological experiments with hopping humans infer that humans choose hopping frequency to maximise effect of stretch reflex [18] and that H reflex suppression during landing changes muscular behaviour from spring to damper [19].

While in human hopping experiments it is difficult to isolate brain signals from lower-level responses, simulations tackle the problem by recreating a simplified version of such experiments. In [20], a simulation of a hopping two-segment leg takes place with muscular activation generated by proprioceptive feedback. In [21, 22], using an opposite approach, simulations adopt a feed forward control, stabilising through irregular terrain while exploiting muscular properties. Haeufle *et al.* [23] suggests a simulation combining feed-forward control with feedback responses, adding disturbances to the simulation and analysing individual contributions from each control alternative.

Real world dynamics involve lots of noise, asymmetries and unknown disturbances, which can not be fully mimicked in simulation environments. Muscular properties are usually approximated by a Hill muscle model [24] and body-environment interactions are usually poor. The field of biomimetics aims to imitate life with artificial systems, allowing experimental settings which thus would not be biologically possible. In [7], an artificial tentacle robot imitates the movements of an octopus, while on [25, 26] a decerebrate biomimetic cat walks on a treadmill with different muscular activations.

In this work, we perform hopping experiments with a robot using artificial pneumatic muscles. Such muscles perform similarly to biological muscles in many aspects (force-length relationship, radial expansion on contraction [8]) thus allow us to analyse stretch reflex contribution during hopping. Different from other bipedal hopping experiments (biological or biomimetic), we evaluate the contribution of stretch reflex on the rolling stability (frontal plane) of humans. Although stretch reflex has been studied in hopping before [27, 28], its contribution to rolling stability has never been approached.

Our biomimetic robot hops in place, landing from different angles and comparing these with their respective lift off angle. We found that stretch reflex improved the lift off angle output. Moreover, hopping with a delay between touching the floor and the stretch reflex response still has better results than the lack of reflex. Performing biomimetic experiments which would be hard to test with humans, this work proves that our body self-stabilizes with lower-level signals, not requiring higher-level inputs to bring the body back to a straight position.

In Chapter 2 we introduce the robot design and the program emulating hopping sequence and stretch reflex. We also describe the experimental setting used to perform experiments. While on Chapter 3 we show experimental results, on Chapter 4 we discuss those results and conclude this work.

2. Methods

Aiming to achieve biologically representative results, the human morphology was replicated considering the musculoskeletal structure with the most representative muscles on human legs. To understand how such muscles interact with the environment, our chosen actuators must mimic their behaviour, thus eliminating electric motors from our design options. Pneumatics and hydraulics are known for offering compliance, with special attention to air muscles, which have been used for many years as a successful replacement for biological muscles in robots[5, 6, 25] and rehabilitation [29].

2.1. Air muscle consideration

When power-to-weight ratio, durability and dynamic behaviour come in consideration, air muscles offer the closest characteristics to human muscles. They can work by intaking air from a pneumatic valve, which creates a contraction effect, while the opposite relaxing effect is created when the air leaves the same. With a power-to-weight ratio of 400:1, the force provided by such muscles is proportional to internal air pressure and muscular deformation [6], as shown in the following equation:

$$F \propto \frac{P}{\Delta l / L_0}$$

where F is the force, P is the internal pressure, L_0 is the relaxed length and Δl is the deformation after muscular activation. According to [30], force-length relationship of these actuators is very close to biological muscles, with higher force outputs being generated by higher activation pressures and longer muscles. We adopted over-the-counter 200mm air muscles (Mckibben Muscle 200, Hitachi Medical Co.) and used non-deformable nylon braided ropes to connect origin and insertion points to the muscle.

2.2. Robot design

The robot has eight air muscles on each leg, from which three are biarticulars and five are monoarticulars, controlling three degrees of freedom in each leg. With an overall weight of 7.8 kg, height of 1.3 m and a 200 mm width, it is depicted in Fig. 1. All the muscles, with exception of tibialis anterior and iliopsoas, are the most important extensors of human legs, acting over ankle, knee and hip.

A passive artificial actuator was placed in parallel with the muscle soleus, acting as a stretch sensor (hence called soleus sensor), detecting muscle deformation. With the intent of producing a lightweight testing platform, the robot uses light materials on its body, such as magnesium alloy, carbon fibre and ABS plastic. The pneumatic valves, micro controller and battery are located inside the torso of the robot, connected by a tether which communicates and supplies compressed air. Two small air tanks act as pneumatic capacitors, offering pressure stability between jumps. The micro controller communicates at 200Hz, powered by a 32-bits 72MHz ARM micro controller (STM32F103, ST Microelectronics), while sampling data from touch sensors at the tip

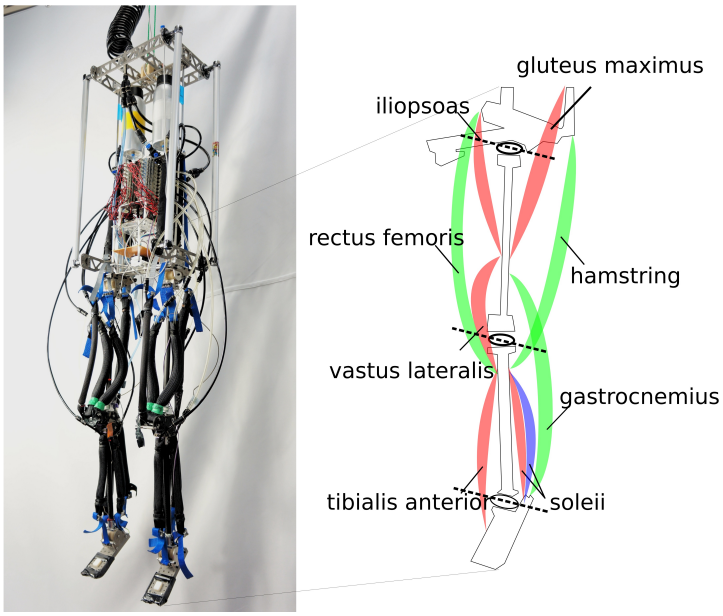

Figure 1. Picture of robot with pictogram detailing muscles on each leg. The robot has pneumatic valves, micro controller and battery on board, and the leg structure has biarticular muscles in green and monoarticular muscles in red, controlling three degrees-of-freedom. Soleus sensor (blue), in parallel with the muscle, has the sole purpose of detecting pressure differences during landing.

of each limb, pressure sensors on each soleus sensor, a three axis accelerometer and two gyroscopes. All these sensors act, respectively, to identify the moment the robot touches the floor, the ankle deformation on landing and to provide roll angle information through a complementary filter between accelerometers and gyroscopes. More information on the robot specifics (human based leg lengths and moment arms) and sensing are located in the appendix A.

2.3. Hopping algorithm

To generate a hopping sequence the robot must be capable of interacting with the environment. Upon touching the floor, the robot should wait for the lowest point to be reached, supplying air to extensor muscles. After lifting off, the robot restores the pressure to the initial landing configuration, preparing for another hop. This way, the hopping is produced by a finite-state machine where three states are present, as shown in Fig. 2:

- Landing state: In the landing state, the robot adjusts the muscular pressure on every muscle to reach a predetermined value, which is the same on every landing condition. This state is the initial state of every experiment.
- Complying state: When the robot detects the touch of the foot against the floor (change of signals on touch sensor) the complying state is activated. In this state, the robot initially waits for a delay (T_d, which is 15 ms for delayed cases, zero

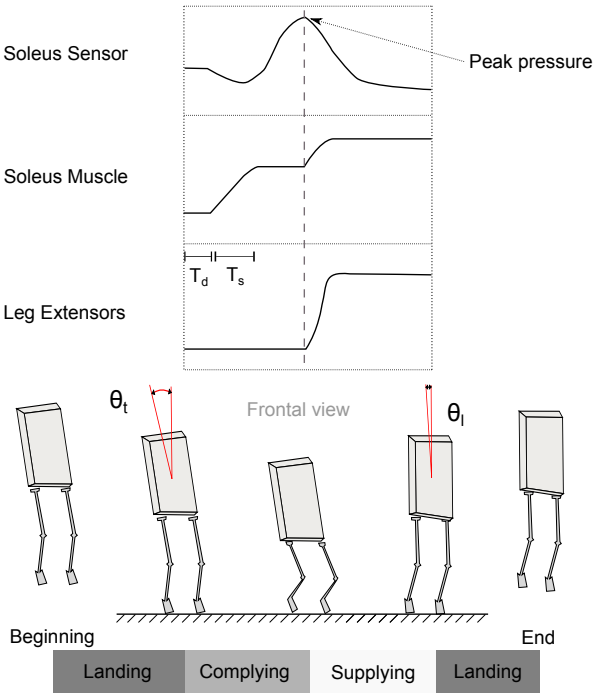

Figure 2. Pictogram of robot performing one experimental cycle. Initially falling in the Landing state, the robot touches the floor with a touch down angle θ_t. Upon touching the floor, the robot transits to the Complying state, awaiting for a delay (T_d) to supply air to the muscle soleus for an specific time (T_s). When the pressure at soleus sensor reaches its peak, the robot transits to Supplying state, contracting all extensors to lift off, registering the lift off angle θ_l and returning to the initial Landing state.

otherwise) and then supplies air to the muscle soleus for a predetermined time (T_s) and closes the muscle. The end of this state is reached when the pressure inside soleus sensor reaches its peak, which is described as:

$$\frac{\partial P_s}{\partial t} = 0$$

where P_s is the muscle pressure inside soleus muscle. The peak in the pressure curve means that the maximum deformation was achieved, activating the next state.

- Supplying state: During this state the major extensor muscles are activated, generating an upward movement. The timing sequence of each muscle during explosion is detailed in previous publications [5], and the landing state is activated after the robot loses contact with the floor, which will once again adjust the muscles for landing.

During hopping, data from roll angle, hopping state and internal pressure on muscles are sampled to a computer. The finite state programming allows right and left legs to respond independently to the floor.

The predetermined time of muscular activation (*e.g.*, $T_s = 30$ would supply soleus for 30 ms, closing the valve after that) can be adjusted, and a second timer, called delay

timer (T_d), can be added to simulate a delay between the trigger and the muscle response. The stretch reflex is modeled as a constant contraction, reacting upon sensing the floor, probing different stretch responses (contraction strengths) on landing to imitate the contraction observed on humans. The main reason for this approach, instead of a reaction proportional to the ground reaction force, is the low precision from these sensors upon impact on the floor, with values fluctuating drastically. The parallel soleus sensor is equally affected when the muscles contract, being unfeasible to contract as the muscle deforms.

Hopping experiments were performed by releasing the robot on the floor from many different attack angles, forcing the robot to develop the three different states mentioned above. One single experimenter was adopted for every trial, using the same pitch attack angle for every jump and releasing the robot from approximately the same height of 25 cm between foot and floor. The experimenter was instructed to drop the robot from random initial roll angles (without any angular velocity or acceleration), where both touching down angle θ_t and lift off angle θ_l are compared after the jump. After the contact between the robot and the floor was lost, the experimenter was instructed to grab the robot midair and prepare to release the robot from another random roll angle.

The results are compared by plotting the initial touch down angle θ_t in the horizontal axis and the lift off angle θ_l in the vertical axis. Since we are interested in measuring the recovering capability of the system, jumps will be graded by the following procedure:

$$X = \begin{cases} \theta_t - \theta_l & \text{if } \theta_t \geq 0 \\ \theta_l - \theta_t & \text{otherwise} \end{cases}$$

where positive values indicate recoveries and negative values indicate worsen conditions. Special attention should be paid to values close to the straight position (0°), since in this region results close to $\Delta_\theta = 0$ would mean that hopping stability is being kept.

During hopping, the position of the centre of gravity (COG) is very important to determine the possibility of rolling stabilisation, where a COG located outside the area below both feet should make stabilisation impossible without abduction. Considering the COG height of 780 mm and distance between feet of 200 mm, $\theta_{max} = \arcsin(100/780) = 7.36°$ is the angle at which the COG would fall entirely on one foot. The hopping range between $-5°$ and $5°$ was chosen, assuring that stretch reflex contribution could be evaluated while allowing individual analysis within five groups: ($-5°$,$-3°$), ($-3°$,$-1°$), ($-1°$,$1°$), ($1°$,$3°$) and ($3°$,$5°$).

Aiming to better understand the contribution from stretch reflex, initial experiments were performed with five different cases: No reflex ($T_s = 0$ms), Reflex-30 ($T_s = 30$ms), Reflex-70 ($T_s = 70$ms), Reflex-100($T_s = 100$ms) and Reflex-130 ($T_s = 130$ms), simulating different reflex strengths upon touching the floor.

The mean and standard deviations of five angle groups from nine different cases were taken, resulting in 45 different groups to be compared. A two-tailed unpaired Student t-test with a 95% confidence interval was used whenever a pairwise comparison

was made, while an one-way ANOVA test with a Bonferroni correction was used for multiple comparisons. Variance ratios were compared to F values and variances do not differ significantly. This approach was chosen over an inclination analysis of a linear regression (such as least squares estimation) for allowing individual analysis of groups, where asymmetry can be properly represented.

3. Results

In Fig. 3 the results of five different hopping experiments are shown. Each of these experiments had more than 100 jumps (top right corner of graphs), and means were calculated for each case in the proposed five different groups (red crosses). Starting from the No Reflex condition, we could notice a degree of linearity among the means (red crosses), where jumps to both sides maintain the same orientation (a). Upon adopting Reflex-30, it is noticed that the inclination of the results decreases (b), approaching the horizontal axis. As a consequence, results for Δ_θ increase (f-g), with more hops passing the $\Delta_\theta = 0$ threshold. Different reflex cases (70ms, 100ms and 130ms) were also tested and their results plotted (c-e). It was found that the trend kept true, with values approximating even more the horizontal axis. Although hopping height was not evaluated, the experimenter observed that increasing the reflex response degraded this height, where the Reflex-130 case had the worst hopping height.

Literature on human stretch reflex [11] shows that a delay between the muscular excitation and the reflex response exists. Based on previous experiments, four new conditions were created, considering $T_d = 15ms$ as a delay between touching the floor and the stretch reflex response: Delay-30, Delay-70, Delay-100 and Delay-130. In Fig. 4, these four new conditions are compared with the previous No Reflex condition. Similarly to previous experiments, the No Reflex case had the highest inclination, with every other case being closer to the horizontal axis. Once again, the performance of Delay-130 was the worst among delayed cases when it comes to hopping height, and the experimenter added that it was worse than Reflex-130.

During the first experimental phase (Fig. 3), it was possible to notice that as the reflex response increased, the inclination of the line formed by the means decreased. A comparison between the means of the performance of each jump (Δ_θ) with their respectives standard deviations is shown in Fig. 5. As it can be seen, an increase in the stretch reflex strength creates a similar effect on the hopping performance Δ_θ. The trend that exists from No Reflex to Reflex-30 (only jumps between $(-3°,-1°)$ are statistically significant, with t=4.02) is reinforced by the comparison between No Reflex and Reflex-100, which is only non-significant between $-1°$ and $1°$. Moreover, Reflex-100 is proven to be the best case, where the case Reflex-130 degrades stretch reflex response in both extremities ($(-5°,-3°)$ and $(3°,5°)$, t = 2.769 and t = 3.491).

In Fig. 6 we can see a comparison based on results shown in Fig. 4. Similarly to the previous comparison, cases No Reflex, Delay-30, Delay-100 and Delay-130 are compared for the same five angle groups. Initially, a comparison between No Reflex and

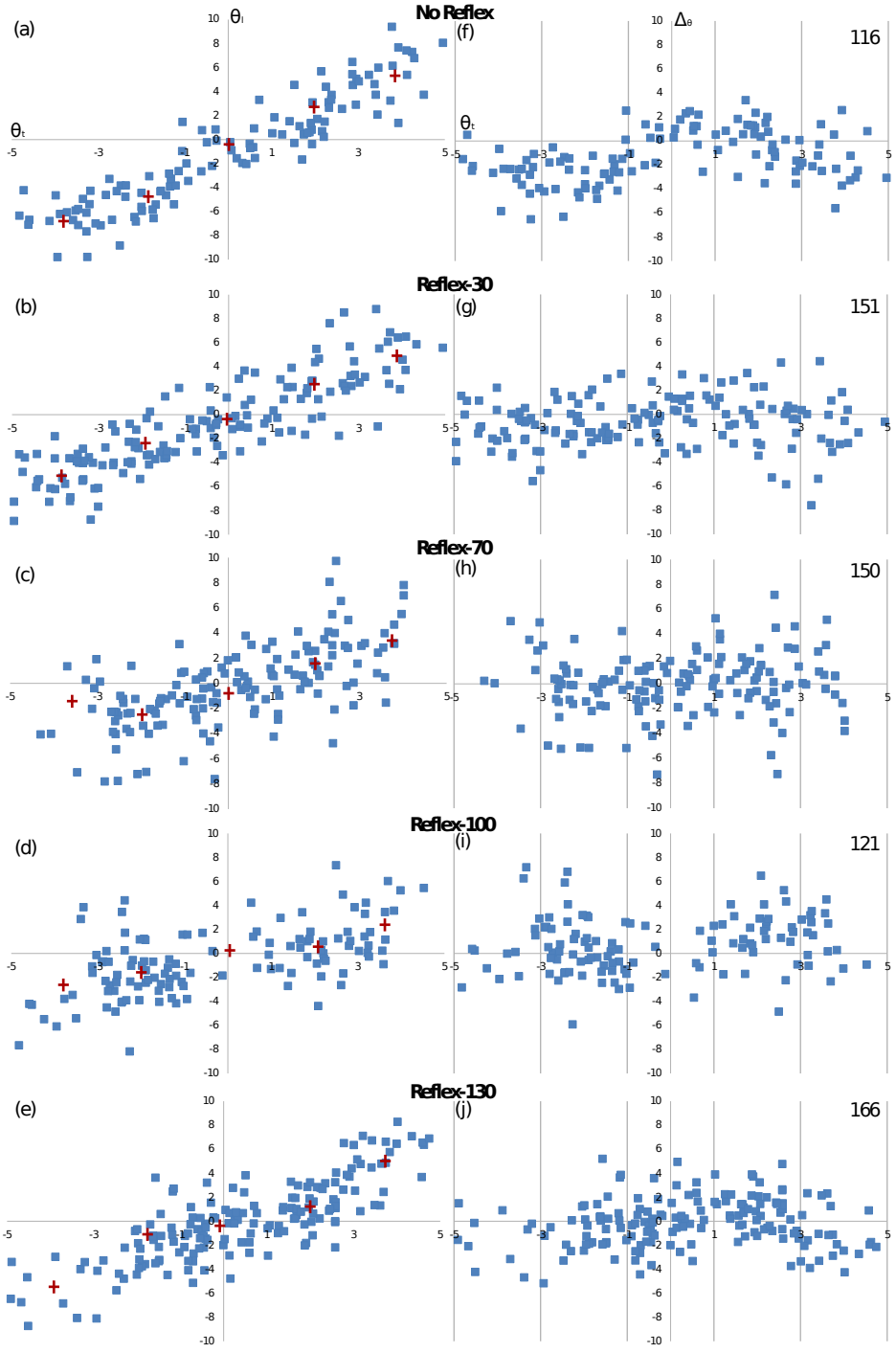

Figure 3. Hopping experiments result, where on the left side (a-e) we have θ_t versus θ_l and on the right side (f-j) we have a performance evaluation with θ_t versus Δ_θ. As the stretch reflex gets stronger, the inclination of the lines passing through the mean points (red crosses) decrease (a-d), increasing again at the Reflex-130 case (e). As a consequence, the number of points above the $\Delta_\theta = 0$ line increases, where initially on the No Reflex (f) case the majority of points is negative and in the best case, Reflex-100 (i), most of its points are above the axis.

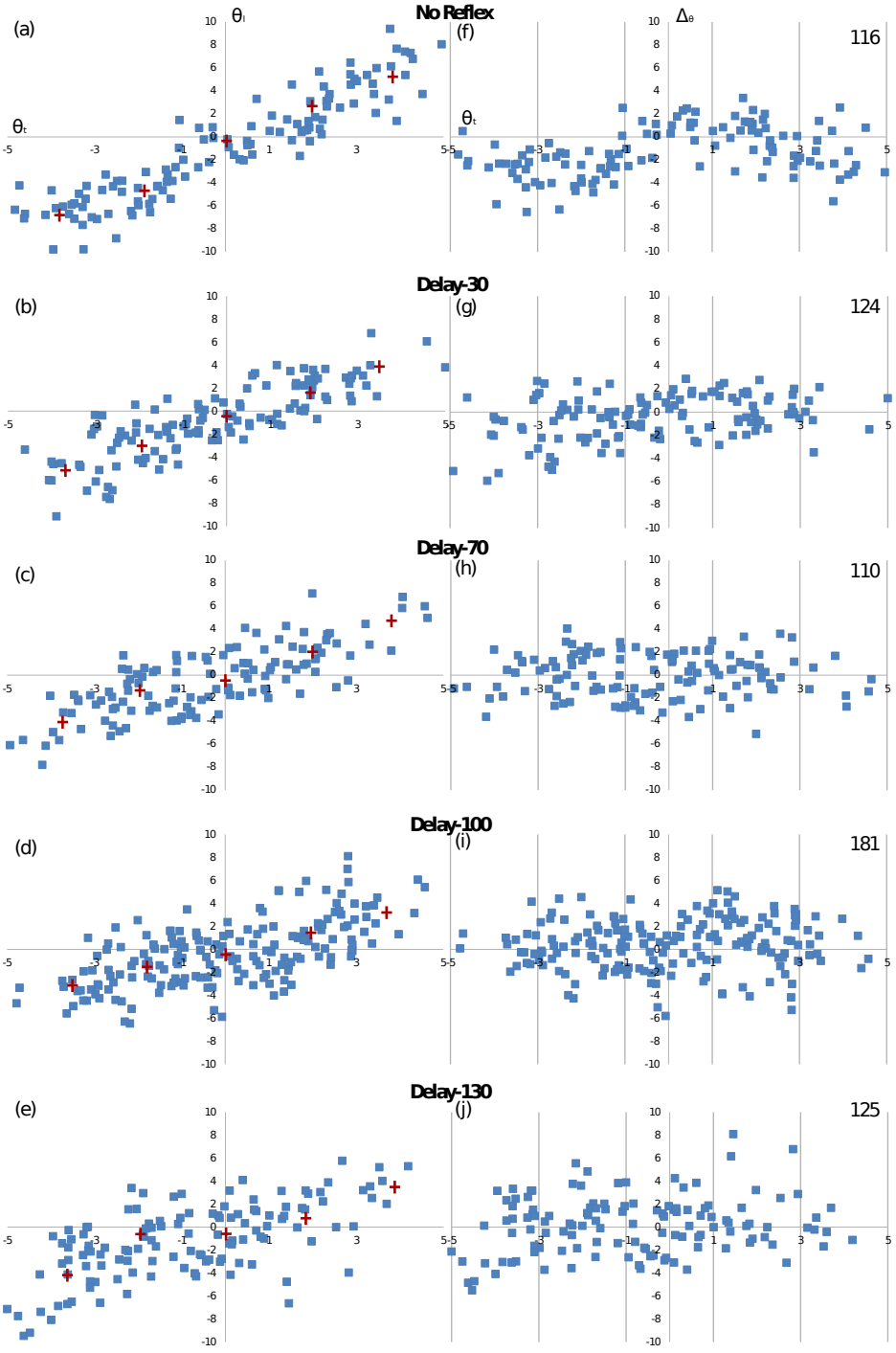

Figure 4. Hopping experiments considering a 15 ms delay before reflex onset, where on the left side (a-e) we have θ_t versus θ_l, and on the right side (f-j) we have a performance evaluation with θ_t versus Δ_θ. As the stretch reflex gets stronger, the inclination of the lines passing through the mean points (red crosses) decrease (a-e). As a consequence, the number of points above the $\Delta_\theta = 0$ line increases, where initially on the No Reflex (f) case the majority of points is negative and in the cases Delay-100 (i) and Delay-130 (j) we can see the best results.

Delay-30 yields only one statistically significant Bonferroni comparison ($(-3°,-1°)$, t = 2.468) with the delayed case outperforming the former. Since mean values from Delay-30 indicated superiority when compared to No Reflex, a stronger case (Delay-100) was also compared to the No Reflex case.

One final comparison between results from Figs. 3 and 4 is regarding which might be the superior case. As seen in Fig. 7, we compared Reflex-30 and Reflex-100 against Delay-30 and Delay-100 to understand if the presence of a delay may degrade roll stability.

4. Discussion

An analysis of stretch reflexes during bipedal hopping has been done clinically [11, 18] and mathematically [22, 23], but none of these researchers considered the stability contribution to the frontal plane. The importance of such reflexes in roll angle stability (frontal plane) goes beyond human hopping, being also applied to bipedal standing, walking and direction change, rarely studied from a low-level feedback perspective. Results obtained through biomimetic experiments can be used in the future to fortify biological hypothesis, providing insight in a field restricted by scarce biological evidence.

The fact that separating brain signals from muscular feedback responses during hopping is clinically difficult explains why such topic is rarely approached in biological experiments. In simulation environments, on the other hand, approaching this topic could be possible by simulating muscular responses with different landing angles on a frontal plane. Although possible, the lack of real world disturbances in this approach would make a physical experiment the best candidate to realistically reproduce observed phenomena. The idea of an unstable biped system applying a harder push off on one leg to restore stability is very trivial, not being the focus of this research. Here, the authors show a possible explanation of "how" this push off is generated, not requiring visual or vestibular (angle) inputs, solely relying on muscle signals to correct posture.

4.1. Stretch reflex improves rolling stability

Analysing results from Fig. 5, which are based on Reflex case data (Fig. 3), a few discussions arise from these comparisons. Although the claim that the presence of the COG closer to one leg would allow a bigger reaction force in the opposite direction is true, such effect is also present during the No Reflex case. While bipeds have this advantage over monopods, this does not explain the superiority from Reflex versus No Reflex cases. We hypothesise that the physical explanation for this phenomenon is that the body, without any brain-generated signal nor pitch/roll information, corrects rolling by activating leg muscles through reflex response upon touching the floor. The implications of this assertion would be that *decerebrate animals, if capable of hopping in place*, would have a frontal plane stabilisation facilitated by such mechanisms.

Analysis of variance between the four cases showed a strongly significant difference

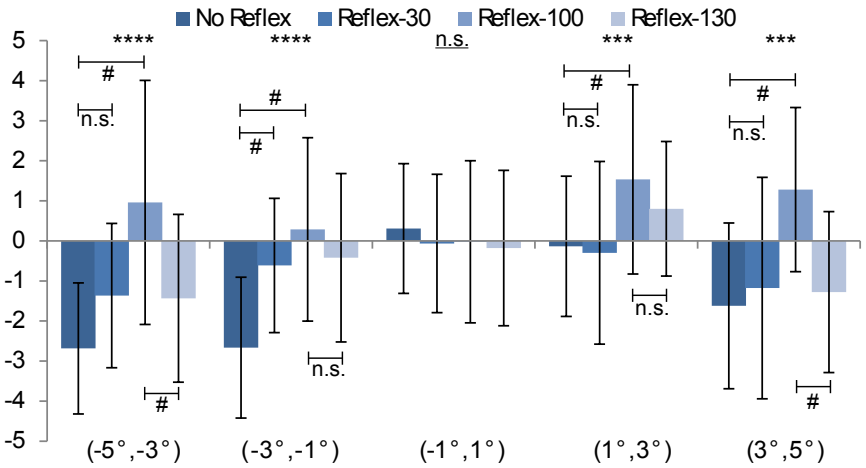

Figure 5. Comparison of Δ_θ performances between No Reflex, Reflex-30, Reflex-100 and Reflex-130 for five proposed angle groups. Higher means indicate better hopping performances. Error bars denote standard deviations. The symbols represent $p < 0.001$ (***), $p < 0.0001$(****) and n.s. for non-significant in ANOVA tests, being $p < 0.05$ (#) and n.s. for non-significant at subsequent Bonferroni correlations.

($p < 0.001$ and $p < 0.0001$) between them for both sides. In Reflex-30 case, only one group ($-3°$,$-1°$) showed statistically significant results. Robotic asymmetry may play a role on this, since both legs are not equal, and its effects on the experiment will be discussed in *Study limitations*. The Reflex-130 case was inferior to the Reflex-100 in both extremities, being non-significant in the middle zone. A possible explanation is that an extremely long reflex activation period interferes with the complying phase, resulting in a smaller amount of stored gravitational energy. In analogy with a spring, Reflex-130 behaved as an overstiff spring which could not bounce properly, not correcting the posture.

In [19], the reflex suppression is compared to a damping unit. Although apparently diverging from our findings, where small reflexes created higher jumps, those results are actually convergent, since during landing (without a posterior jump) the stored energy is dissipated. Thus, the hypothesised damping unit must be associated with a soft spring, being the damper suppressed in case of a countermovement jump (involving stretching muscles, similar to our No Reflex case and well described in [31]). During hopping, both results converge to a higher muscle stiffness produced by reflexes.

While hopping within ($-1°$,$1°$) range is very interesting when control stability is desired, this region did not yield good results when studying roll angle correction through stretch reflex. Small angles allow the robot to hop in random directions, and the need for rolling correction does not exist. Regarding the adopted grading system (Δ_θ), a higher mean found in No Reflex (not statistically significant) may not indicate superiority over Reflex cases. Whenever the robot hops close to the straight position, changing hopping directions can be seen as an overcompensated recovery measure, and in this aspect $\Delta_\theta = 0$ might be a more desirable output. More experiments with continuous hops, evaluating the long-term influence on the system will be performed.

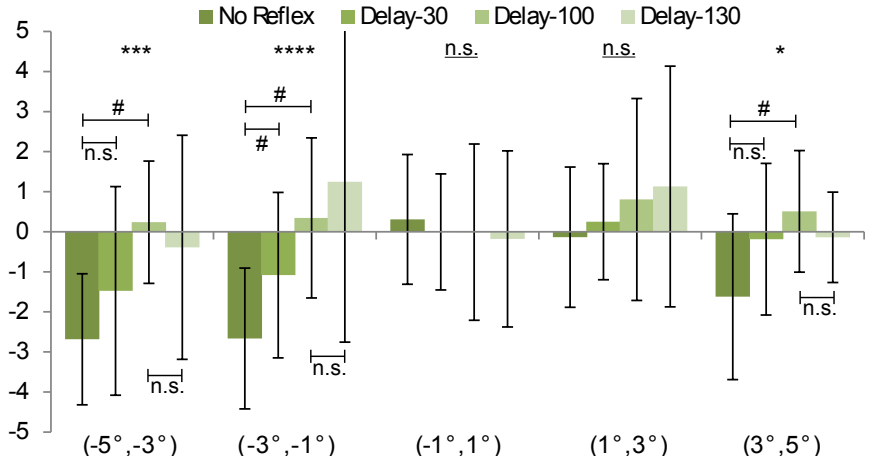

Figure 6. Comparison of Δ_θ performances between No Reflex, Delay-30, Delay-100 and Delay-130 for the 5 proposed angle groups. Higher means indicate better hopping performance. Error bars denote standard deviations. The symbols represent $p < 0.05$ (*), $p < 0.001$(***), $p < 0.0001$(****) and n.s. for non-significant in ANOVA tests, being $p < 0.05$ (#) and n.s. for non-significant at subsequent Bonferroni correlations.

4.2. Delay presence outperforms lack of reflex

Observing Delay case results from Fig. 6, a strong significance ($p < 0.001$ and $p < 0.0001$) was found for one side entirely ($-5°$,$-1°$), while for the other only the region ($3°$,$5°$) had $p < 0.05$. Hence, the stretch reflex corrective behaviour still holds true when a delay is applied, similarly to human beings. Although human stretch reflex is greater than 15 ms (in [11] values between 30 and 40 ms can be seen), this value was used considering the intrinsic delay of air muscles. Upon opening pneumatic valves, compressed air takes longer than a biological soleus muscle to reach its peak force, adding a latency to the response.

Similarly to the previous Reflex case comparison, the region ($-1°$,$1°$) once again had a higher mean (not statistically significant) for No Reflex than any other case, requiring more experiments to clarify hopping stability when landing in a straight position.

As observed by the experimenter, the case Delay-130 had the worst hopping performance. Recalling an analogy to the spring made in the previous section, the case Delay-130 acts as a very soft spring for 15 ms, complying with the gravitational force, and suddenly stiffening for 130 ms. Although clearly superior to the No Reflex case in roll angle correction aspects, this unnatural hopping strategy produced a very small ground clearance while hopping. Comparisons between this case and Delay-100 were inconclusive, with all cases being statistically non-significant.

4.3. Delayed versus undelayed cases

Finally, in Fig. 7 we perform a comparison between Reflex and Delay cases. As observed previously, Reflex-130 had a better hopping height performance when compared to Delay-130 cases, and a possible explanation is the sudden change between soft and

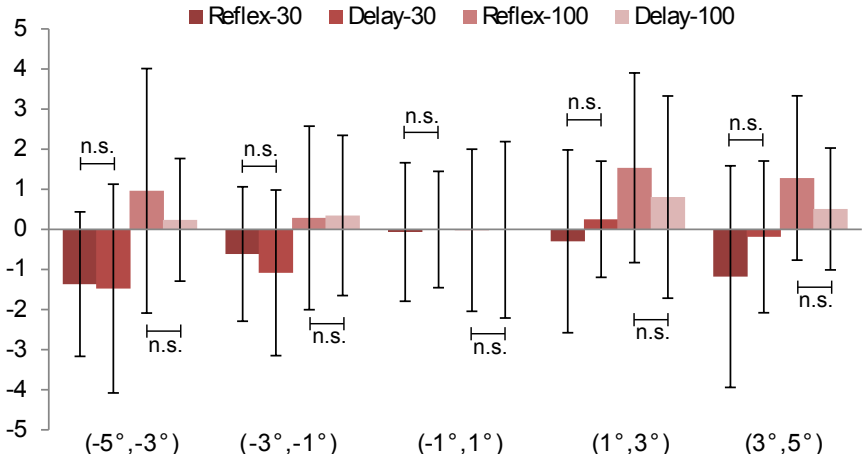

Figure 7. Comparison of Δ_θ performances between Reflex-30, Delay-30, Reflex-100 and Delay-100 for the 5 proposed angle groups. Higher means indicate better hopping performance. Error bars denote standard deviations. Due to proximity of means/high standard deviation all pairwise comparisons were considered non-significant (n.s.) in t-tests for a 95 % confidence interval. One-tailed comparisons would have rendered the same non-significance.

hard spring behaviours.

Statistically, it was not possible to determine which case had superiority over the other, with all comparisons being non-significant. Analysing mean values from comparisons between cases (Fig. 7), we may observe that all the cases in the range $(-1°,1°)$ performed similarly, which also holds true for No Reflex cases. As discussed before, mean values close to $\Delta_\theta = 0$ may represent a better stability than higher values. The non-significance shown in previous sections compels us to perform more experiments in the future, clarifying this issue.

The mean values for Reflex-30 cases are superior to Delay-30 cases' means for hops to one side (negative region, $p = 0.86$ and $p = 0.30$), while Delay-30 means are superior in the opposite direction (positive region, $p = 0.24$ and $p = 0.39$). Reflex-100 cases' means are superior to Delay-100 cases in almost all hops ($p = 0.42$, 0.20 and 0.29), being the only exception the $(1°,3°)$ range ($p = 0.89$). Even if a one-tailed approach was adopted prior to the beginning of experiments, no presumption could have been made against the null hypothesis. Future experiments will be performed, suggesting new conditions to better assess the effect of a delay on the stretch reflex. Both Reflex and Delay cases performed better than the No Reflex case, but it remains unclear which one is the best.

4.4. Study limitations and conclusion

As any experiment where biological conditions are recreated artificially, our experiments had some study limitations. Air muscles are considered, so far, the best replacement, but they are not biological muscles. During hopping, muscle contraction rate is high,

and forces exerted by air muscles are not affected by contraction speed, differently from biological muscles (force-velocity relationship degrades force with increasing velocity). Moreover, the time to reach peak force in pneumatic muscles is higher than biological ones, hence the shorter delay used (15 ms).

Although differences between air and biological muscles exist, results obtained in this work hint that phenomena observed here will also be observed biologically, perhaps in different proportions, and may also be replicated with different types of actuation. Future biological experiments should address, if possible, the mechanisms explained here to observe how they affect animal locomotion.

Robotic asymmetry was mentioned throughout this paper, with some phenomena being observed on one side and not holding true for the other. We believe that a perfectly symmetrical robot could have reproduced phenomena equally for both sides, but that is not the purpose of this work. The presence of asymmetry is not a limitation *per se*, specially when such feature is also present in humans and other bipeds. Instead of facing asymmetric data (non-significant to one side, significant to the other) as a failed experiment, we believe that this should be understood as an additional source of disturbance on the hopping system, common in real life experiments, fortifying our findings.

It is clear that the contribution from a higher-level control (brain) on our stability is high. Even so, understanding how much our body contributes to locomotion is essential to understand biological systems and, in the future, use this information to understanding locomotion, develop prosthetics or legged robots for everyday use. In this work, the presence of stretch reflexes helped frontal plane stabilisation in a biomimetic humanoid, and adding a delay to the reflex response did not degrade this phenomenon. The contribution of stretch reflexes in decerebrate animals is explained from a novel perspective, helping us understand the self-stability present in animals.

In the future, experiments with decerebrate animals (deprived from vestibular and visual feedback) falling from a platform in different angles could help reproduce this work from a biological aspect, if feasible. Whenever biological experiments are constrained by their own inner workings, biomimetic experiments emerge as the best interface between computer simulations and clinical trials.

5. Appendix A. Detailed Robotic Design

The construction of the robot involved a milling machine (MDX-540, Roland Corporation) and a 3d Printer (Connex260, Objet Geometries Ltd.), among other hand-cut materials. A list of main specs can be found in Table 1. The construction aimed to mimic the musculoskeletal structure of human beings, including maximum moment arms (Fig. 8).

Touch sensors were made by using force-sensing resistors (FSR-406, Interlink Electronics) in a voltage divider with a 7.5 kΩ resistor, with the chosen touch threshold being 1.2 V. The adopted pneumatic valves (VQZ1321, SMC Corporation) connect to

Table 1. Jumping Robot specs

Parameter	Value
Shoulder-Hip Distance	630mm
Hip-Knee Distance	360mm
Knee-Ankle Distance	340mm
Inter-feet Distance	200mm
COG height	780mm
Weight	7.8 kg
Hip range of motion	$-45°$˜$90°$
Knee range of motion	$-120°$˜$0°$
Ankle range of motion	$-60°$˜$60°$
Air muscle contraction rate	30%
Air muscle length	200mm

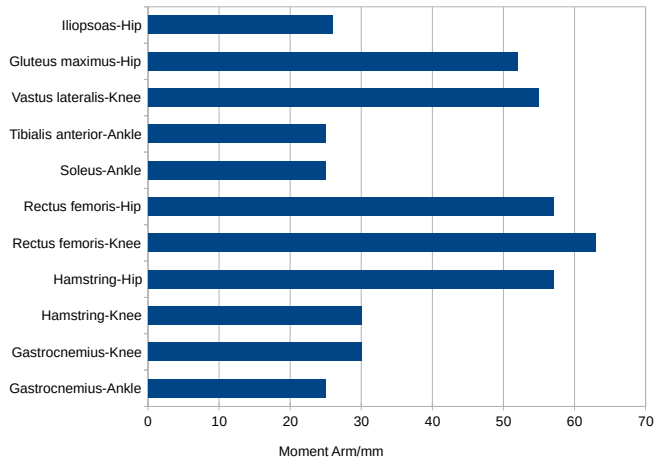

Figure 8. Graph with maximum moment arms used during robot construction.

the muscles, having a pressure sensor (PSE540, SMC Corporation) connected between them. All the valves exhaust to the room and are supplied by a compressor (2000-40m, Jun Air) through a tether. A three DOF accelerometer (KXR94, Kionix Inc.) and two gyroscopes (CRS03, Silicon Sensing Systems) are combined in a complementary filter to generate roll and pitch angle information.

The complementary filter adopted to register roll angle during jumping used gyroscope (1 axis) and accelerometer (2 axis) to create an estimation of roll angle. Initially, both Y and Z axis of the accelerometer were used to find an angular projection in the frontal plane, using:

$$\Theta_{a(x,n)} = arctan(y/z)$$

where y and z are the coordinates of the force vector registered by the accelerometer and $\Theta_{a(x)}$ is the angular position around the X axis, according to accelerometer at instant n.

The gyroscope, on the other hand, registers angular velocity, and thus uses a previous angular estimation to update itself:

$$\Theta_{g(x,n)} = \Theta_{e(x,n-1)} + \dot{\Theta}_{g(x,n)}T$$

where T is the sample period. This way, with both contributions from accelerometer and gyroscope, the new estimate is calculated:

$$\Theta_{e(x,n)} = \frac{\Theta_{a(x,n)} + w\Theta_{g(x,n)}}{1+w}$$

where w is the weight, which in this case was 90.

References

[1] Muybridge R. 1888 *Animal locomotion: the Muybridge work at the University of Pennsylvania.* Ann Arbor, MI: University of Michigan Press.

[2] Engberg I, Lundberg A. 1969 An electromyographic analysis of muscular activity in the hindlimb of the cat during unrestrained locomotion. *Acta Physiol Scand.* **75**, 614-630.

[3] Goslow Jr. GE, Reinking RM, Stuart DG. 1973 The cat step cycle: hind limb joint angles and muscle lengths during unrestrained locomotion. *J Morphol.* **141**, 1-42.

[4] Daley M. 2008 Biomechanics: Running over uneven terrain is a no-brainer. *Current Biol.* **18**, 1064-1066.

[5] Hosoda K, Sakaguchi Y, Takayama H, TakumaT. 2010 Pneumatic driven jumping robot with anthropomorphic muscular skeleton structure. *Auton. Robot.* **28**, 307-316.

[6] Boblan I, Bannasch R, Schwenk H, Prietzel F, Miertsch L, Schulz A. 2004 *Embodied Artificial Intelligence.* Dagstuhl Castle, Germany: Springer.

[7] Calisti M, Giorelli M, Levy G, Mazzolai B, Hochner B, Laschi C, Dario P. 2011 An octopus-bioinspired solution to movement and manipulation for soft robots. *Bioinsp. Biomim.* **6**, 036002.

[8] Azizi E, Roberts TJ. 2013 Variable gearing in a biologically inspired pneumatic actuator array. *Bioinsp. Biomim.* **8**, 026002

[9] Paul C, Belloti M, Jezernik S, Curt A. 2005 Development of a human neuro-musculo-skeletal model for investigation of spinal cord injury. *Biol. Cybern.* **93**, 153-170.

[10] Fibley RA, Gazzaniga MS. 1969 Splitting the normal brain with reaction time. *Psychonomic Science.* **17**, 335-336.

[11] Voigt M, Chelli F, Frigo C. 1998 Changes in the excitability of soleus muscle short latency stretch reflexes during human hopping after 4 weeks of hopping training. *Eur. J. Appl. Physiol..* **78**, 522-532.

[12] Pearson K, Ekeberg O, Buschges A. 2006 Assessing sensory function in locomotor systems using neuro-mechanical simulations. *Trends in Neurosciences.* **29**, 625-630.

[13] Hiebert GW, Pearson KG. 1999 Contribution of sensory feedback to the generation of extensor activity during walking in the decerebrate cat. *J. Neurophysiol..* **81**, 758-770.

[14] Kukillaya R, Proctor J, Holmes P. 2009 Neuromechanical models for insect locomotion: Stability, maneuverability, and proprioceptive feedback. *Chaos.* **19**, 026107.

[15] Fallon JB, Bent LR, McNulty PA, Macefield VG. 2005 Evidence for strong synaptic coupling between single tactile afferents from the sole of the foot and motoneurons supplying leg muscles. *J. Neurophysiol.* **94**, 3795-3804.

[16] Carpenter MG, Allum JHJ, Honegger F. 1999 Directional sensitivity of stretch reflexes and balance corrections for normal subjects in the roll and pitch planes. *Exp. Brain Res.* **129**, 93-113.

[17] Sinkjaer T, Andersen JB, Larsen B. 1996 Soleus stretch reflex modulation during gait in humans. *J. Neurophysiol.* **76**, 1112-1120.

[18] Melvil Jones G, Watt DGD. 1971 Observations on the control of stepping and hopping movements in man. *J. Physiol.* **219**, 709-727.

[19] Dyhre-Poulsen P, Simonsen EB, Voigt M. 1991 Dynamic control of muscle stiffness and H reflex modulation during hopping and jumping in man. *J. Physiol.* **437**, 287-304.

[20] Geyer H, Seyfarth A, Blickhan R. 2003 Positive force feedback in bouncing gaits. *Proc. R. Soc. Lond. B* **270**, 2173-2183.

[21] van der Krogt MM, de Graft WW, Farley CT, Moritz CT, Casius LJR, Bobbert MF. 2009 Robust passive dynamics of the musculoskeletal system compensate for unexpected surface changes during human hopping. *J. Appl. Physiol.* **107**, 801-808.

[22] Haeufle DFB, Grimmer S, Seyfarth A. 2010 The role of intrinsic muscle properties for stable hopping - stability is achieved by the force-velocity relation. *Bioinsp. Biomim.* **5**, 016004.

[23] Haeufle DFB, Grimmer S, Kalveram KT, Seyfarth A. 2012 Integration of intrinsic muscle properties, feed-forward and feedback signals for generating and stabilizing hopping. *J. R. Soc. Interface* **9**, 1458–1469.

[24] Perreault EJ, Heckman CJ, Sandercock TG. 2003 Hill muscle model errors during movement are greatest within the physiologically relevant range of motor unit firing rates. *J.Biomech.* **36**, 211–218.

[25] Rosendo A, Nakatsu S, Narioka K, Hosoda K. 2014 Producing alternating gait on uncoupled feline hindlimbs: muscular unloading rule on a biomimetic robot. *Advanced Robotics* **28**, 351–365.

[26] Rosendo A, Nakatsu S, Narioka K, Hosoda K. 2013 Pneupard: A biomimetic musculoskeletal approach for a feline-inspired quadruped robot. In *Proc. IEEE Int. Conf. Int. Robots and Sys., IROS 2013, Tokyo, Japan, 3-7 Nov 2013*. Piscataway, NJ: IEEE.

[27] van Soest J, Bobbert MF. 1993 The contribution of muscle properties in the control of explosive movements. *Biol. Cybern.* **69**, 195–204.

[28] Maie H, Oida Y, Kitabatake Y, Egawa K. 2001 Effect of hopping tempo on stretch-reflex of function soleus muscle at landing phase. *Jpn. J. Phys. Fitness Sports Med.* **50**, 139–148.

[29] Xie SQ, Jamwal PK. 2011 An iterative fuzzy controller for pneumatic muscle driven rehabilitation robot. *Expert Systems with Applications.* **38**, 8128–8137.

[30] Klute G, Czerniecki J, Hannaford B. 2002 Artificial muscles: Actuators for biorobotic systems. *Int. J. Robotics Res.* **21**, 295–309.

[31] Alexander RMN. 1995 Leg design and jumping technique for humans, other vertebrates and insects. *Phil. Trans. R. Soc. Lond. B.* **347**, 235–248.